

Attention-guided Feature Distillation for Semantic Segmentation

Amir M. Mansourian*, Arya Jalali*, Rozhan Ahmadi, Shohreh Kasaei

Sharif University of Technology

amir.mansurian, arya.jalali79, roz.ahmadi, kasaei@sharif.edu

Abstract

In contrast to existing complex methodologies commonly employed for distilling knowledge from a teacher to a student, this paper showcases the efficacy of a simple yet powerful method for utilizing refined feature maps to transfer attention. The proposed method has proven to be effective in distilling rich information, outperforming existing methods in semantic segmentation as a dense prediction task. The proposed Attention-guided Feature Distillation (AttnFD) method, employs the Convolutional Block Attention Module (CBAM), which refines feature maps by taking into account both channel-specific and spatial information content. Simply using the Mean Squared Error (MSE) loss function between the refined feature maps of the teacher and the student, AttnFD demonstrates outstanding performance in semantic segmentation, achieving state-of-the-art results in terms of improving the mean Intersection over Union (mIoU) of the student network on the PascalVoc 2012, Cityscapes, COCO, and CamVid datasets.

Introduction

Semantic segmentation is a highly important and challenging task in computer vision. It has become an integral component in various applications; such as autonomous driving, video surveillance, and scene parsing. Its goal is to perform dense prediction by assigning a specific class label to each pixel in the image. Semantic segmentation has witnessed significant advancements through the use of deep neural networks, led by Fully Convolutional Network (FCN) (Long, Shelhamer, and Darrell 2015). Other methods have consistently improved the segmentation accuracy by building on FCN. They achieve this by employing strategies such as designing deeper architectures to increase the capacity of FCN (Zhao et al. 2017), incorporating stronger backbones (Huang et al. 2017), and hierarchical image context processing (Fu et al. 2019). Increasing the complexity is effective in improving the accuracy of semantic segmentation, yet it has become a rising concern in resource-limited environments; such as mobile and edge devices.

In recent years, many studies have focused on designing lightweight models with lower computational costs that

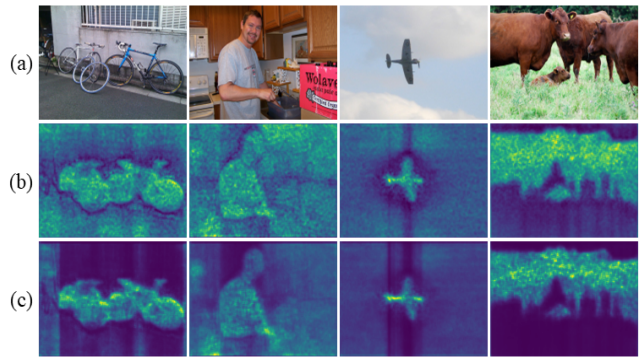


Figure 1: Visualization of images (a), raw feature maps (b), and refined feature maps (c). Channel and spatial attention is applied to raw features, emphasizing on the important regions and making them valuable distillation source.

are suitable for real-world applications. For example, they achieve efficiency through making the complex backbone networks lighter by reducing the number of convolutional layers or completely replacing the backbone with a simpler model. Among these methods, the Knowledge Distillation (KD) has proven to be an effective strategy for optimizing the balance between accuracy and efficiency in deep neural networks. This technique distills useful information from a larger (teacher) network and leverages this knowledge to supervise the training of a lighter (student) network. While KD is beneficial for image classification, it faces challenges in enhancing semantic segmentation task due to its limited ability in capturing contextual correlation among pixels.

As research progresses, there has been a shift towards feature-based distillation and aligning intermediate feature maps between teacher and student networks. To achieve this, many methodologies have proposed complex loss functions to enhance knowledge distillation, since replicating feature maps with simple distance measures had limitations. While these methods are effective, recent studies (Liu et al. 2023; Yang et al. 2022b; Zagoruyko and Komodakis 2016) suggest that transforming student feature maps through novel modules while retaining basic loss functions can lead to simpler networks with improved performance.

*These authors contributed equally.

Attention mechanism is designed to mimic the way humans view a visual scene. In fact, instead of processing the complete image at once, humans tend to select areas with important information to pay more attention to (by ignoring other parts of the image). Given attention’s capability to aggregate long-range contextual semantic information, its integration into feature-based KD holds promise for significant impact. Despite its potential, this approach has currently remained largely unexplored.

Unlike previous works, which either define complex losses to consider pairwise relations or rely on raw features, this study leverages the attention mechanism in CBAM(Woo et al. 2018). This mechanism incorporates both channel and spatial information to produce refined features, which are then distilled from the teacher to the student. Figure 1 illustrates the distinction between raw and refined features. As depicted in this figure, the refined feature highlights important regions of the image and reduces background noise, making it a strong candidate with significant potential for distillation. This is because it compels the student network to mimic the important regions emphasized by the teacher.

A summary of the main contributions of this work includes:

- Investigating the role of attention mechanisms in feature-based distillation methods for semantic segmentation.
- Proposing a novel and simple attention-based feature distillation method using the CBAM attention module. This is the first work to use both channel and spatial attention in the context of knowledge distillation.
- Validating the effectiveness of the proposed method by comparing it to existing state-of-the-art methods across four widely used benchmarks with two different network architectures.

Related Work

A literature review of state-of-the-art studies relevant to the proposed method is presented in this section. It contains discussions on KD and attention mechanism.

Knowledge Distillation

Initially introduced in (Hinton et al. 2015), the concept of KD is to minimize the Kullback-Leibler Divergence between probability maps of the teacher and the student. Subsequently, various paradigms emerged. Fitnet (Romero et al. 2014) extracts and aligns feature maps from the hidden layers of a network. In (Zagoruyko and Komodakis 2016) the student undergoes training to emulate the corresponding intermediate attention map from the teacher. The RKD (Park et al. 2019) involves extracting distance and angle-based correlations between feature maps. The work in (Peng et al. 2019) presents a framework to balance the correlation and instance compatibility between samples. The (Zhao et al. 2021) provides the student model with a softer sample distribution through a mixture of input samples. On the other hand, certain studies attempt to improve the KD through various tricks, such as employing an adaptive cross-entropy loss function (Park and Heo 2020), reducing the duration

of distillation’s impact (Zhou et al. 2020; Mansourian, Ahmadi, and Kasaie 2023), pruning features before the distillation process (Park and No 2022) or investigating the role of projectors and temperature in KD (Miles and Mikolajczyk 2024; Li et al. 2023).

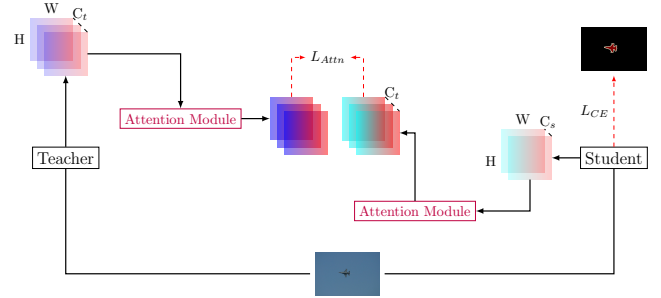


Figure 2: Proposed Attention-guided feature distillation.

Knowledge Distillation for Semantic Segmentation For semantic segmentation, which requires high-level information, more advanced forms of knowledge distillation have been proposed, such as adversarial training (Liu et al. 2019) and prototyping (Wang et al. 2020). Furthermore, different similarity distillation methods have been proposed at various levels, including instance-level (Tung and Mori 2019), class-level (Feng et al. 2021; Huang et al. 2022), and channel-level (Park and Heo 2020; Liu et al. 2021). More recently, additional forms of relationships have been considered. The CIRKD (Yang et al. 2022a) extracts relations across images to capture a better global knowledge about pixel dependencies. The BPKD (Liu et al. 2024a) uses separate distillation loss functions for body and edge to improve edge differentiation.

Although these methods have proven to be effective, their novel ways of defining and distilling the knowledge usually result in complex models that require prior knowledge and careful feature extraction processes. As a result, some studies have gravitated towards designing modules to transform features and extract rich information from them. The proposed method in MGD (Yang et al. 2022b) involves masking random pixels of the student’s feature and training it to replicate the feature of the teacher. Some recent works have also showcased improved performance by using the raw features directly or through simple transformations. The MLP (Liu et al. 2023) achieves this by aligning features across their channel dimension, using a simple channel-wise transformation. The DiffKD (Huang et al. 2024) treats the student’s feature maps as a noisy version of the teacher’s feature maps, and trains a diffusion model to refine the student’s features for more effective knowledge distillation. The LAD (Liu et al. 2024b) demonstrates that using the MSE loss between raw features of the teacher and the student can significantly improve the performance.

Attention Mechanism

This mechanism allows models to extract local context information from an image more accurately (Vaswani et al.

2017). Some methods, such as SE-NET (Hu, Shen, and Sun 2018) and SGE-NET (Li, Hu, and Yang 2019), calculate attention at the inter-channel level, and Self-attention (Ambartsoumian and Popowich 2018) considers pair-wise similarity of the input’s pixels. The BAM (Park et al. 2018) calculates channel and spatial attention and CBAM (Woo et al. 2018) performs spatial attention after channel-wise attention. Recently, EMA(Ouyang et al. 2023) have proposed an efficient multi-scale attention by channel grouping. In the context of KD, (An et al. 2022) utilizes an attention mechanism by incorporating the concept from (Fu et al. 2019) and employing spatial self-attention for the distillation process.

In this work, we employ the CBAM attention mechanism to refine raw features, as it adaptively performs the spatial and channel attention. To the best of our knowledge, this is the first instance of utilizing both channel and spatial attention for the purpose of knowledge distillation.

Methodology

This section first reviews feature distillation and then presents the details of our proposed method.

Revisiting Feature Distillation

In feature distillation, the student network is trained to mimic the teacher’s feature maps:

$$L_{fd} = \ell_{feat}(\Phi_s(F_s), \Phi_t(F_t)) \quad (1)$$

where ℓ_{feat} is a similarity function for matching the teacher’s (F_t) and student’s (F_s) features, and Φ is a transformation used to align the feature size and channels if there is an inconsistency.

Recent studies have suggested using more sophisticated transformations (Φ_s, Φ_t) to not only align feature sizes, but also to better enable student network to acquire knowledge from teacher network. For instance, MLP (Liu et al. 2023) utilizes a simple channel transformation, and DiffKD (Huang et al. 2024) proposes a diffusion model for feature denoising. This research direction raises the question of whether the use of well-designed transformation is necessary for student network to learn more effective features from the teacher.

This work conducts empirical studies to address the aforementioned question, and finds that student model can boost its representations through an attention transformation. Leveraging this insight, as shown in Figure 2, we introduce a straightforward method that integrates a Convolutional Block Attention Module (CBAM) (Woo et al. 2018) into the student and teacher features, and aligns the refined student features with the refined teacher features using a conventional MSE distance. The following sections first describe the CBAM module and then detail our proposed Attention-guided Feature Distillation (AttnFD) approach.

Convolutional Block Attention Module

Let $F \in \mathbb{R}^{c \times w \times h}$ be an intermediate feature map obtained from the student or the teacher network with spatial and channel dimensions of $h \times w$ and c , respectively. Two attention modules aggregate spatial ($M_S(F) \in \mathbb{R}^{c \times h \times w}$) and

channel descriptors ($M_C(F) \in \mathbb{R}^{c \times 1 \times 1}$) of an intermediate feature. These spatial and channel attention descriptors are then multiplied by the original feature map F to create new rich context feature maps F' and F'' , introducing inter-channel and inter-spatial information into the original feature map. The overall formulation of feature refinement is given by

$$F' = M_C(F) \otimes F \quad (2)$$

$$F'' = M_S(F') \otimes F' \quad (3)$$

where \otimes is the element-wise multiplication. During multiplication, spatial attention maps are broadcasted along the channels, and channel attention maps are broadcasted along the spatial dimensions. The methodology of the channel and spatial attention modules can be seen in Figure 3 and Figure 4, respectively.

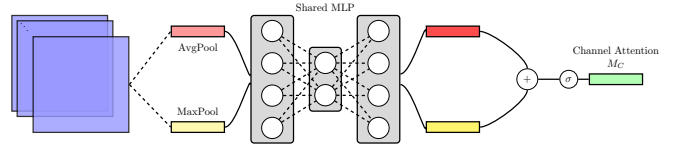


Figure 3: Channel Attention Module. It applies average-pooling and max-pooling operators along the channel dimension. Resulting outputs are then passed through a shared Multi-Layer Perceptron and fed into a sigmoid activation function to generate the channel attention map M_C .

Channel Attention Module The Channel Attention Module (CAM) aggregates spatial information by applying the max-pooling and average-pooling operators to an intermediate feature map F . These operations produce context descriptors, which are then processed by a multi-layer perceptron to generate a channel attention map $M_C(F)$. This map highlights the meaningful regions of the image while obscuring regions that are irrelevant to the segmentation task, such as the background. The channel-aware descriptors for an intermediate feature map F are defined by

$$M_C(F) = \sigma(W_1(W_0(F_{\text{avg}}^C)) + W_1(W_0(F_{\text{max}}^C))) \quad (4)$$

where $F_{\text{avg}}^C \in \mathbb{R}^{c \times 1 \times 1}$ and $F_{\text{max}}^C \in \mathbb{R}^{c \times 1 \times 1}$ are the feature maps generated by applying the average-pooling and max-pooling operators to the intermediate feature map F . The W_1 and W_0 are the weights of the shared MLP between the two pooled feature maps. The W_0 is followed by a ReLU activation function, and σ denotes the sigmoid function.

Spatial Attention Module The Spatial Attention Module (SAM), shown in Figure 4, operates fairly similar to CAM. Spatial information of an intermediate feature map F are aggregated by using the max and average pooling operators to generate two different spatial context descriptors $F_{\text{avg}}^S \in \mathbb{R}^{1 \times h \times w}$ and $F_{\text{max}}^S \in \mathbb{R}^{1 \times h \times w}$. Then, the spatial context descriptors for F are calculated as

$$M_S(F) = \sigma(A^{7 \times 7}([F_{\text{avg}}^S; F_{\text{max}}^S])) \quad (5)$$

where $A^{7 \times 7}$ represents a 7×7 convolution kernel.

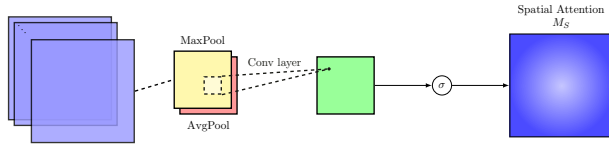


Figure 4: Spatial Attention Module. Max-pooling and average-pooling operators are utilized to generate feature descriptors. These descriptors are subsequently fed into a convolution layer and a sigmoid activation function, resulting in spatial attention map M_S .

Table 1: Quantitative results on PascalVoc Validation set.

Method	mIoU(%)	Params(M)
T: DeepLabV3-Res101	77.85	59.3
S: DeepLabV3-Res18	67.50	
S + KD	69.13 ± 0.11	
S + DistKD	69.84 ± 0.11	16.6
S + CIRKD	71.02 ± 0.11	
S + LAD	71.42 ± 0.09	
S + AttnFD (ours)	73.09 ± 0.06	
S: DeepLabV3-MBV2	63.92	
S + KD	66.39 ± 0.21	
S + DistKD	67.62 ± 0.22	5.9
S + CIRKD	69.02 ± 0.16	
S + LAD	68.63 ± 0.07	
S + AttnFD (ours)	70.38 ± 0.16	
S: PSPNet-Res18	67.4	
S + KD	68.18 ± 0.08	
S + DistKD	68.93 ± 0.19	12.6
S + CIRKD	69.53 ± 0.11	
S + LAD	69.71 ± 0.10	
S + AttnFD (ours)	70.95 ± 0.06	

Attention-guided Feature Distillation

Using the newly acquired features, the proposed loss is calculated as

$$L_{Attn} = \frac{1}{N} \sum_{i=1}^N \left\| \frac{F''_{Sj}}{\|F''_{Sj}\|} - \frac{F''_{Tj}}{\|F''_{Tj}\|} \right\| \quad (6)$$

where F''_{Sj} and F''_{Tj} represent the j 'th intermediate context-rich feature map for the student and teacher network, respectively. Each feature map is normalized along its channels before calculating the difference matrix.

The overall loss function is then a weighted sum of L_{CE} and L_{Attn} , given by

$$L_{AttnFD} = L_{CE} + \alpha L_{Attn} \quad (7)$$

where α is a weight coefficient which is fine-tuned as described in next section. In this context, the well-known cross-entropy loss function, L_{CE} , is employed as the segmentation loss between the predictions of the student network and the ground-truth labels.

Experimental Results

Datasets and Evaluation Metrics

(1) **Cityscapes** (Cordts et al. 2016) dataset, designed for understanding urban scenes, includes 2975/500/1525 images for train/val/test, covering 19 classes. (2) **PascalVOC** (Everingham et al. 2010) dataset comprises 1464/1449/1456 images for train/val/test, with 21 classes. (3) **COCO** (Everingham et al. 2010) dataset is a large-scale dataset, containing 118K/5K/41K labeled images for the train/val/test sets, across 91 classes. (4) **CamVid** (Brostow, Fauqueur, and Cipolla 2009) is a road scene understanding dataset with a total of 701 labeled video frames, including 367/101/233 images for train/val/test sets, in 11 classes.

Evaluation Metrics As per the standard, segmentation performance is evaluated using the mIoU and pixel accuracy, averaged over three runs for fair comparison. The model size is indicated by the reported number of network parameters.

Implementation Details

Network Architecture To ensure impartial assessment, the experiments employ identical teacher and student networks as described in (Liu et al. 2021). The teacher network consistently applied across all experiments is DeepLab V3+ with ResNet101 serving as the backbone. Various backbones, such as ResNet18 and MobileNetv2, are utilized for the student network within the DeepLab V3+ and PSPNet segmentation networks.

Training Details All the datasets utilize similar configurations for training the student networks. For the Pascal and CamVid datasets, a batch size of 6 and a total of 120 epochs are employed, whereas for the Cityscapes dataset, a batch size of 4 and a total of 50 epochs, and for the COCO dataset, a batch size of 6 and a total of 10 epochs are utilized. The Stochastic Gradient Descent (SGD) optimizer is employed with an initial learning rate set to 0.007 for Pascal, 0.01 for Cityscapes, 0.1 for COCO, and 0.02 for CamVid. The learning rate adjustment is performed based on the cosine annealing scheduler. Before the training phase, each image undergoes preprocessing, including random scaling between 0.5 to 2 times its original size, horizontal random flipping, and random cropping to dimensions of 513×513 pixels for Pascal and COCO, 512×1024 for Cityscapes, and 360×360 for CamVid. The backbones of both the teacher and student networks utilize pre-trained weights from the ImageNet dataset, while the segmentation parts are initialized randomly. The only hyperparameter of the method described in equation 7 was fine-tuned by experimenting with values $\{0.1, 1, 10, 100\}$ for finding proper value, and then trying with some different numbers around it for finding the best value. It was established as $\alpha = 2$ for the Pascal, COCO, and CamVid datasets, and $\alpha = 15$ for the Cityscapes dataset. During inference, performance is assessed on original inputs at a single scale. Instead of utilizing raw feature maps, Pre-ReLU feature maps are employed, as suggested in (Heo et al. 2019), to retain negative values for applying attention module. The implementation is in PyTorch framework, with all networks trained on a single NVIDIA GeForce RTX 3090 GPU.

It is important to highlight that any inconsistency in the size and number of channels of features between the teacher and the student is addressed through the interpolation and inclusion of a convolutional layer respectively. Additionally, the parameters of the teacher and its attention module are trained and then frozen during the training of the student.

Comparison with state-of-the-art methods

Extensive experiments were conducted to assess the performance of the proposed AttnFD. It was compared against several existing distillation methods; namely, KD (Hinton et al. 2015), CIRKD (Yang et al. 2022a), DistKD (Huang et al. 2022), and LAD (Liu et al. 2024b). Each of the aforementioned methods underwent testing across all backbone, encoder, and decoder features, as well as final output maps, to determine the optimal results.

PascalVoc. Initially, the outcomes of the proposed method are compared with those of the aforementioned methods on the PascalVoc dataset. As illustrated in Table 1, AttnFD demonstrates notable performance enhancement for the model without distillation, achieving a 5.59% increase when employing ResNet18 as the student backbone, and a 6.46% improvement with MobileNet as the student backbone. Moreover, our method surpasses the top-performing existing methods by a significant margin. Specifically, it outperforms LAD by 1.67% with ResNet18, and CIRKD by 1.36% with MobileNet as the student backbone, positioning it as the second-best method. Furthermore, AttnFD outperforms LAD by 1.24% in performance when a student model with a PSPNet architecture is employed, demonstrating that the proposed method is architecture-independent and can effectively enhance the performance of various model architectures. Qualitative comparisons based on ResNet18 are depicted in Figure 5.

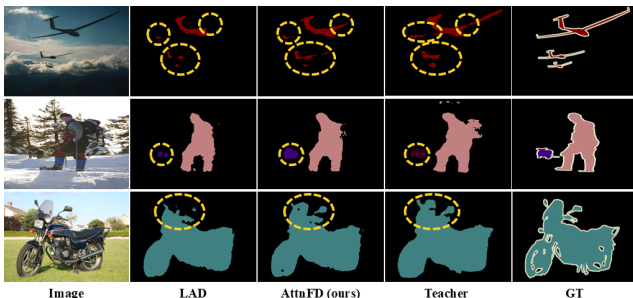


Figure 5: Some qualitative comparisons on the PascalVoc validation split.

Cityscapes. The proposed method underwent evaluation on the Cityscapes dataset alongside existing methods. Quantitative results presented in Table 2 indicate that AttnFD enhances the performance of ResNet18, MobileNet, and PSPNet students by 8.95%, 7.75%, and 3.14% respectively. Notably, compared to DistKD and LAD, the second-best methods, AttnFD surpasses them by 1.23%, 0.96%, and 0.73% respectively in terms of mIoU. Additionally, it demonstrates improvements in pixel accuracy, enhancing DistKD and

LAD by 2.08%, 1.1%, and 0.22% respectively. The qualitative comparisons utilizing ResNet18 with DistKD validate the efficacy of the proposed method, as depicted in Figure 6.

COCO. Similar to the results on the two previous datasets, Table 3 shows the performance of the AttnFD on the validation set of the COCO dataset. The results demonstrate that AttnFD outperforms the SOTA by 1.18%, 1.66%, and 0.58% when using ResNet18, MobileNet, and PSPNet as the student networks, respectively.

CamVid. As shown in Table 4, the proposed AttnFD method outperforms existing techniques on both the validation and test sets of the CamVid dataset. The results demonstrate that AttnFD achieves superior performance when using either DeepLab (ResNet18) or PSPNet (ResNet18) as the student networks.

Table 2: Quantitative results on Cityscapes Validation set.

Method	mIoU(%)	Accuracy(%)
T: DeepLabV3-Res101	77.66	84.05
S: DeepLabV3-Res18	64.09	74.8
S + KD	65.21 (+1.12)	76.32 (+1.74)
S + CIRKD	70.49 (+6.40)	79.99 (+5.19)
S + DistKD	71.81 (+7.72)	80.73 (+5.93)
S + LAD	71.37 (+7.28)	80.93 (+6.13)
S + AttnFD (ours)	73.04 (+8.95)	83.01 (+8.21)
S: DeepLabV3-MBV2	63.05	73.38
S + KD	64.03 (+0.98)	75.34 (+1.96)
S + CIRKD	69.34 (+6.39)	78.66 (+5.28)
S + DistKD	69.53 (+6.48)	79.10 (+5.72)
S + LAD	69.84 (+6.79)	80.49 (+7.11)
S + AttnFD (ours)	70.80 (+7.75)	81.59(+8.15)
S: PSPNet-Res18	65.72	73.77
S + KD	66.89 (+1.17)	74.82 (+1.05)
S + CIRKD	67.51 (+1.79)	75.25 (+1.48)
S + DistKD	68.13 (+2.41)	76.25 (+2.48)
S + LAD	67.71 (+1.99)	75.63 (+1.86)
S + AttnFD (ours)	68.86 (+3.14)	76.47 (+2.70)

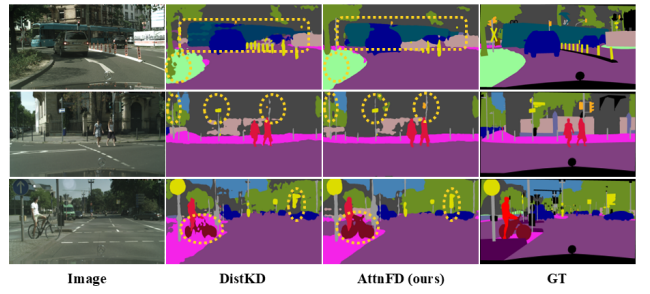


Figure 6: Enhancements in visual quality on Cityscapes validation set.

Table 3: Quantitative results on COCO Validation set.

Method	Params (M)	mIoU(%)
T: DeepLabV3-Res101	59.3	60.56
S: DeepLabV3-Res18		52.08
S + KD		54.6
S + CIRKD	16.6	55.60
S + DistKD		55.9
S + LAD		56.56
S + AttnFD (ours)		57.74
S: DeepLabV3-MBV2		47.92
S + KD		52.21
S + CIRKD	5.9	53.65
S + DistKD		53.33
S + LAD		55.29
S + AttnFD (ours)		56.95
S: PSPNet-Res18		52.68
S + KD		54.07
S + CIRKD	12.6	56.96
S + DistKD		55.06
S + LAD		57.50
S + AttnFD (ours)		58.08

Ablation Study

To further affirm the effectiveness of the proposed method, ablation studies were conducted. Since the method focuses on minimizing the MSE loss between the refined feature maps of the teacher and students, we explored the impact of these feature maps across different layers of the network. Table 5 presents the results for three distinct feature maps: "B," which denotes low-level features acquired by the network's backbone, "E," representing features obtained from the last layer of the encoder, and "D," indicating the feature map just before the final convolutional layer of the network. As evidenced by the results, all these features contribute to improved performance, as observed for both ResNet18 and MobileNet backbones on the PascalVoc dataset. Notably, the features from the Decoder exhibit more pronounced improvements compared to those from the Encoder, and both surpass the features from the Backbone. This is attributed to the richer, more detailed information contained in the network's final layers. When combined, all three features collectively achieve the best performance.

Figure 7 illustrates the per-class mIoU comparison between AttnFD and LAD on the PascalVoc dataset, utilizing ResNet18 for the student. As depicted, AttnFD performs roughly on par or slightly better than LAD, with notable performance improvements in specific classes, such as bicycle (+10.1), sheep (+5.96), bird (+4.85), and chair (+4.1). As illustrated in the first column of Figure 1, the attention maps produced by the proposed method exhibit a stronger focus on the bicycle compared to the raw feature maps, while containing significantly less noise. Furthermore, the visualization of the attention maps and feature maps in the third column demonstrates how the attention mechanism effectively

Table 4: Quantitative results on CamVid dataset.

Method	Val mIoU(%)	Test mIoU(%)
T: DeepLabV3-Res101	76.02	65.35
S: DeepLabV3-Res18	71.20	62.89
S + CIRKD	76.20	67.58
S + DistKD	75.36	68.32
S + LAD	76.13	66.57
S + AttnFD (ours)	76.39	68.77
S: PSPNet-Res18	72.64	63.02
S + CIRKD	73.89	65.03
S + DistKD	75.96	65.09
S + LAD	75.84	66.13
S + AttnFD (ours)	76.56	66.74

directs more focus towards the main object (the cow) rather than the background, thereby reducing the likelihood of detecting backdoors when segmenting the object.

In a similar vein, Figure 8 presents a comparison on the Cityscapes dataset between AttnFD and DistKD (also using ResNet18 as the student). AttnFD demonstrates significantly superior performance in classes like train (+12.91) and bus (+2.82). The top row of Figure 6 corroborates this, highlighting DistKD's misclassification of the bus as a train, a mistake rectified by AttnFD's improved performance. Moreover, AttnFD exhibits better segmentation of traffic lights and traffic signs compared to DistKD. This improvement can be attributed to the enhanced highlighting of tiny objects like traffic lights in the refined feature maps, which aids the student in mimicking the teacher's attention more effectively, resulting in better segmentation of small objects.

Table 6 presents an ablation study on the different attention modules used for the proposed attention-guided feature distillation on PascalVod validation set. This table provides the mIoU improvement, a brief explanation, and the number of learnable parameters for each attention module, namely: Attention Transfer (AT) (Zagoruyko and Komodakis 2016), Self-Attention (SA) (Ambartsumian and Popowich 2018), Bottleneck Attention Module (BAM) (Park et al. 2018), Efficient Multi-Scale Attention (EMA) (Ouyang et al. 2023), and Convolutional Block Attention Module (CBAM) (Woo et al. 2018).

The results show that the SA module contains significantly more learnable parameters, making it more memory-consuming during the training phase. In contrast, the EMA module has the lowest number of parameters (AT module has no learnable parameters at all). However, the CBAM module strikes a balanced trade-off between mIoU improvement and the number of parameters, consistently achieving better results than the other attention modules. CBAM learns to automatically consider both pixel-wise and channel-wise information, which are two important sources of information that have been investigated in the literature for the purpose of knowledge distillation.

Table 5: An ablation analysis conducted on PascalVOC validation set, examining the influence of distilling refined feature maps across various layers of the network.

Method	mIoU(%)	Accuracy(%)
T:DeepLabV3-Res101	77.85	-
S:DeepLabV3-Res18	67.50	76.49
S + B	70.25 (+2.75)	78.88 (+2.39)
S + E	72.31 (+4.81)	81.48 (+4.99)
S + D	72.47 (+4.97)	82.13 (+5.64)
s + B + E	72.58 (+5.08)	81.71 (+5.22)
S + B + D	72.82 (+5.32)	81.87 (+5.38)
S + E + D	72.92 (+5.42)	82.68 (+6.19)
S + B + E + D	73.09 (+5.59)	82.95 (+6.46)
S:DeepLabV3-MBV2	63.92	73.98
S + B	66.68 (+2.76)	77.01 (+3.03)
S + E	68.91 (+4.99)	79.60 (+5.62)
S + D	69.55 (+5.63)	78.50 (+4.52)
s + B + E	69.17 (+5.25)	79.61 (+5.63)
S + B + D	69.46 (+5.54)	78.65 (+4.67)
S + E + D	69.96 (+6.04)	79.73 (+5.75)
S + B + E + D	70.38 (+6.46)	81.13 (+7.21)

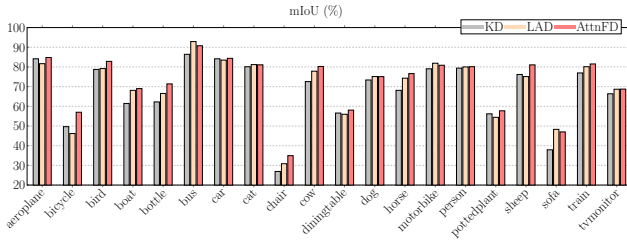


Figure 7: Visual representation of the performance of proposed method in terms of per-class mIoU using ResNet18 network on PascalVoc validation set.

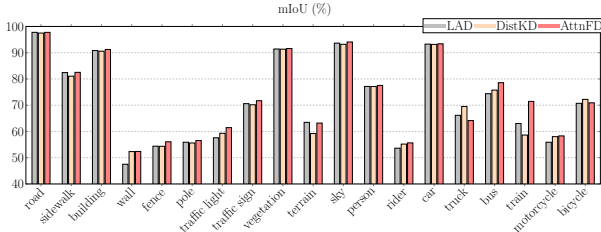


Figure 8: Comparison of mIoU per class among LAD, DistKD, and AttnFD on Cityscapes validation set, employing a ResNet18 backbone for the student network.

Discussion

The proposed method incorporates an additional distillation loss alongside the cross-entropy loss for segmentation. Unlike other existing methods that perform multiple distillation losses, such as the KD loss, it only needs to fine-tune just one hyperparameter. It is worth mentioning that despite our various attempts, combining the proposed method with the KD

loss not only did not yield any enhancement in mIoU but it also slightly decreased it (-0.5%). This indicates that the proposed loss function effectively distills crucial information from the teacher’s refined feature maps to the student. Additionally, per-class mIoU results, shown in Figure 7, demonstrate that AttnFD consistently surpasses or matches the performance of the KD method across all classes, indicating that incorporating KD loss does not offer additional benefits. In contrast, the LAD method exhibits inferior results compared to the KD method in specific classes (like bicycle and aeroplane). This highlights the necessity of utilizing the KD loss to enhance results for these particular classes in the LAD method.

Furthermore, experimentation with reducing the coefficient of our distillation loss towards the end of training, which has been proven to be helpful in (Zhou et al. 2020; Mansourian, Ahmadi, and Kasaei 2023), resulted in a minor decrease in performance. This suggests that the CBAM module effectively learns to highlight crucial information for transfer to the student, supported by Figure 1, which shows refined feature maps with reduced noise and emphasized regions ready for distillation.

Table 6: Ablations for different attention modules.

Method	mIoU(%)	Params	Explanation
S: ResNet18	67.50	-	w/o attention
S + AT	68.95	-	Channel Aggregation w/o learning
S + SA	71.72	492800	Pairwise similarity of pixels
S + BAM	72.68	103235	Simultaneously channel & spatial attention
S + EMA	72.86	3986	Multi-scale attention by channel grouping
S + CBAM	73.09	50540	Channel and then spatial attention
S: MobileNet	63.92	-	w/o attention
S + AT	66.27	-	Channel Aggregation w/o learning
S + SA	68.29	292880	Pairwise similarity of pixels
S + BAM	69.96	61703	Simultaneously channel & spatial attention
S + EMA	70.05	2348	Multi-scale attention by channel grouping
S + CBAM	70.38	30368	Channel and then spatial attention

Conclusion

A novel method for semantic segmentation was introduced. Unlike existing approaches, which often focus on pairwise information or involve complex distillation losses, the proposed method simplified the process by using raw features and applying channel and spatial attention through the convolutional block attention module to refine feature maps. These refined features highlighted crucial image regions and contained rich information for distillation purposes. Extensive experiments on four known benchmark datasets consistently demonstrated significant performance improvements over models without distillation. Comparison with the state-of-the-art methods further validated the effectiveness of the proposed method.

References

Ambartsoumian, A.; and Popowich, F. 2018. Self-attention: A better building block for sentiment analysis neural network classifiers. *arXiv preprint arXiv:1812.07860*.

An, S.; Liao, Q.; Lu, Z.; and Xue, J.-H. 2022. Efficient semantic segmentation via self-attention and self-distillation.

IEEE Transactions on Intelligent Transportation Systems, 23(9): 15256–15266.

Brostow, G. J.; Fauqueur, J.; and Cipolla, R. 2009. Semantic object classes in video: A high-definition ground truth database. *Pattern recognition letters*, 30(2): 88–97.

Cordts, M.; Omran, M.; Ramos, S.; Rehfeld, T.; Enzweiler, M.; Benenson, R.; Franke, U.; Roth, S.; and Schiele, B. 2016. The Cityscapes Dataset for Semantic Urban Scene Understanding. In *Proc. of the IEEE Conference on Computer Vision and Pattern Recognition (CVPR)*.

Everingham, M.; Van Gool, L.; Williams, C. K.; Winn, J.; and Zisserman, A. 2010. The pascal visual object classes (voc) challenge. *International journal of computer vision*, 88(2): 303–338.

Feng, Y.; Sun, X.; Diao, W.; Li, J.; and Gao, X. 2021. Double similarity distillation for semantic image segmentation. *IEEE Transactions on Image Processing*, 30: 5363–5376.

Fu, J.; Liu, J.; Tian, H.; Li, Y.; Bao, Y.; Fang, Z.; and Lu, H. 2019. Dual attention network for scene segmentation. In *Proceedings of the IEEE/CVF conference on computer vision and pattern recognition*, 3146–3154.

Heo, B.; Kim, J.; Yun, S.; Park, H.; Kwak, N.; and Choi, J. Y. 2019. A comprehensive overhaul of feature distillation. In *Proceedings of the IEEE/CVF International Conference on Computer Vision*, 1921–1930.

Hinton, G.; Vinyals, O.; Dean, J.; et al. 2015. Distilling the knowledge in a neural network. *arXiv preprint arXiv:1503.02531*, 2(7).

Hu, J.; Shen, L.; and Sun, G. 2018. Squeeze-and-excitation networks. In *Proceedings of the IEEE conference on computer vision and pattern recognition*, 7132–7141.

Huang, G.; Liu, Z.; Van Der Maaten, L.; and Weinberger, K. Q. 2017. Densely connected convolutional networks. In *Proceedings of the IEEE conference on computer vision and pattern recognition*, 4700–4708.

Huang, T.; You, S.; Wang, F.; Qian, C.; and Xu, C. 2022. Knowledge distillation from a stronger teacher. *Advances in Neural Information Processing Systems*, 35: 33716–33727.

Huang, T.; Zhang, Y.; Zheng, M.; You, S.; Wang, F.; Qian, C.; and Xu, C. 2024. Knowledge diffusion for distillation. *Advances in Neural Information Processing Systems*, 36.

Li, X.; Hu, X.; and Yang, J. 2019. Spatial group-wise enhance: Improving semantic feature learning in convolutional networks. *arXiv preprint arXiv:1905.09646*.

Li, Z.; Li, X.; Yang, L.; Zhao, B.; Song, R.; Luo, L.; Li, J.; and Yang, J. 2023. Curriculum temperature for knowledge distillation. In *Proceedings of the AAAI Conference on Artificial Intelligence*, volume 37, 1504–1512.

Liu, L.; Huang, Q.; Lin, S.; Xie, H.; Wang, B.; Chang, X.; and Liang, X. 2021. Exploring inter-channel correlation for diversity-preserved knowledge distillation. In *Proceedings of the IEEE/CVF International Conference on Computer Vision*, 8271–8280.

Liu, L.; Wang, Z.; Phan, M. H.; Zhang, B.; Ge, J.; and Liu, Y. 2024a. BPKD: Boundary Privileged Knowledge Distillation For Semantic Segmentation. In *Proceedings of the IEEE/CVF Winter Conference on Applications of Computer Vision*, 1062–1072.

Liu, T.; Chen, C.; Yang, X.; and Tan, W. 2024b. Rethinking Knowledge Distillation with Raw Features for Semantic Segmentation. In *Proceedings of the IEEE/CVF Winter Conference on Applications of Computer Vision*, 1155–1164.

Liu, Y.; Chen, K.; Liu, C.; Qin, Z.; Luo, Z.; and Wang, J. 2019. Structured knowledge distillation for semantic segmentation. In *Proceedings of the IEEE/CVF Conference on Computer Vision and Pattern Recognition*, 2604–2613.

Liu, Z.; Wang, Y.; Chu, X.; Dong, N.; Qi, S.; and Ling, H. 2023. A simple and generic framework for feature distillation via channel-wise transformation. In *Proceedings of the IEEE/CVF International Conference on Computer Vision*, 1129–1138.

Long, J.; Shelhamer, E.; and Darrell, T. 2015. Fully convolutional networks for semantic segmentation. In *Proceedings of the IEEE conference on computer vision and pattern recognition*, 3431–3440.

Mansourian, A. M.; Ahmadi, R.; and Kasaei, S. 2023. AICSD: Adaptive Inter-Class Similarity Distillation for Semantic Segmentation. *arXiv preprint arXiv:2308.04243*.

Miles, R.; and Mikolajczyk, K. 2024. Understanding the role of the projector in knowledge distillation. In *Proceedings of the AAAI Conference on Artificial Intelligence*, volume 38, 4233–4241.

Ouyang, D.; He, S.; Zhang, G.; Luo, M.; Guo, H.; Zhan, J.; and Huang, Z. 2023. Efficient multi-scale attention module with cross-spatial learning. In *ICASSP 2023-2023 IEEE International Conference on Acoustics, Speech and Signal Processing (ICASSP)*, 1–5. IEEE.

Park, J.; and No, A. 2022. Prune your model before distill it. In *European Conference on Computer Vision*, 120–136. Springer.

Park, J.; Woo, S.; Lee, J.-Y.; and Kweon, I. S. 2018. Bam: Bottleneck attention module. *arXiv preprint arXiv:1807.06514*.

Park, S.; and Heo, Y. S. 2020. Knowledge distillation for semantic segmentation using channel and spatial correlations and adaptive cross entropy. *Sensors*, 20(16): 4616.

Park, W.; Kim, D.; Lu, Y.; and Cho, M. 2019. Relational knowledge distillation. In *Proceedings of the IEEE/CVF Conference on Computer Vision and Pattern Recognition*, 3967–3976.

Peng, B.; Jin, X.; Liu, J.; Li, D.; Wu, Y.; Liu, Y.; Zhou, S.; and Zhang, Z. 2019. Correlation congruence for knowledge distillation. In *Proceedings of the IEEE/CVF International Conference on Computer Vision*, 5007–5016.

Romero, A.; Ballas, N.; Kahou, S. E.; Chassang, A.; Gatta, C.; and Bengio, Y. 2014. Fitnets: Hints for thin deep nets. *arXiv preprint arXiv:1412.6550*.

Tung, F.; and Mori, G. 2019. Similarity-preserving knowledge distillation. In *Proceedings of the IEEE/CVF International Conference on Computer Vision*, 1365–1374.

Vaswani, A.; Shazeer, N.; Parmar, N.; Uszkoreit, J.; Jones, L.; Gomez, A. N.; Kaiser, Ł.; and Polosukhin, I. 2017. Attention is all you need. *Advances in neural information processing systems*, 30.

Wang, Y.; Zhou, W.; Jiang, T.; Bai, X.; and Xu, Y. 2020. Intra-class feature variation distillation for semantic segmentation. In *Computer Vision–ECCV 2020: 16th European Conference, Glasgow, UK, August 23–28, 2020, Proceedings, Part VII 16*, 346–362. Springer.

Woo, S.; Park, J.; Lee, J.-Y.; and Kweon, I. S. 2018. Cbam: Convolutional block attention module. In *Proceedings of the European conference on computer vision (ECCV)*, 3–19.

Yang, C.; Zhou, H.; An, Z.; Jiang, X.; Xu, Y.; and Zhang, Q. 2022a. Cross-image relational knowledge distillation for semantic segmentation. In *Proceedings of the IEEE/CVF Conference on Computer Vision and Pattern Recognition*, 12319–12328.

Yang, Z.; Li, Z.; Shao, M.; Shi, D.; Yuan, Z.; and Yuan, C. 2022b. Masked generative distillation. In *European Conference on Computer Vision*, 53–69. Springer.

Zagoruyko, S.; and Komodakis, N. 2016. Paying more attention to attention: Improving the performance of convolutional neural networks via attention transfer. *arXiv preprint arXiv:1612.03928*.

Zhao, H.; Gong, K.; Sun, X.; Dong, J.; and Yu, H. 2021. Similarity transfer for knowledge distillation. *arXiv preprint arXiv:2103.10047*.

Zhao, H.; Shi, J.; Qi, X.; Wang, X.; and Jia, J. 2017. Pyramid scene parsing network. In *Proceedings of the IEEE conference on computer vision and pattern recognition*, 2881–2890.

Zhou, Z.; Zhuge, C.; Guan, X.; and Liu, W. 2020. Channel distillation: Channel-wise attention for knowledge distillation. *arXiv preprint arXiv:2006.01683*.